

## Chaotic behavior in the cranking and particles-rotor models

A. T. Kruppa and K. F. Pál

*Institute of Nuclear Research, H-4001 Debrecen, P.O. Box 51, Hungary*

N. Rowley\*

*Department of Physics and Astronomy, University of Manchester, Manchester M13 9PL, United Kingdom*

*and Department of Physics, University of Surrey, Guildford GU2 5XH, United Kingdom*

(Received 12 December 1994)

We investigate the consequences on the order/chaos transition of replacing the scalar rotational energy of the particles-rotor model by a one-body cranking term. The nearest-neighbor distribution of energy levels and the spectral rigidity are studied as a function of the spin or cranking frequency, respectively. Exact energies for our statistical analyses are obtained from a full diagonalization of a many-body Hamiltonian with two-body forces for six particles in an  $i_{13/2}$  shell coupled to a deformed core. In this model, the competing physical effects (two-body interaction strength, quadrupole deformation, and moment of inertia) are easily parametrized and studied. The dependence of the chaoticity on model parameters reveals the stabilizing influence of a large quadrupole deformation. For low spins, the considerable effects of the (effectively two-body) recoil term give significant differences between the two descriptions.

PACS number(s): 24.60.Lz, 05.45+b, 21.60.Ev

### I. INTRODUCTION

The connection between statistical measures of a quantum-mechanical spectrum and the phase-space behavior of the corresponding classical system has been recently revealed. Numerical studies of systems with few degrees of freedom have confirmed that fluctuating properties of quantal systems fall into one of the four universality classes of Dyson and Mehta depending on the space-time symmetries of the Hamiltonian. In the case of nuclei, it is reasonable to assume that time-reversal invariance and rotational symmetry will hold, though many model calculations explicitly break one or both of these symmetries, or indeed others, in the interests of obtaining more tractable calculations.

The short-range correlation between the energy levels is measured by the nearest-neighbor distribution (NND) whereas the long-range correlation is probed by the Dyson-Mehta  $\Delta_3$  statistics (spectral rigidity). Exact numerical calculations and analytical investigations based on semi-classical arguments support the observation that the Gaussian orthogonal ensemble (GOE) and Poissonian spectral statistics are signs of classically chaotic and ordered motion, respectively. For generic systems Berry and Tabor showed [1] that the NND is Poissonian provided that the system is classically integrable (fully ordered). As far as spectral rigidity is concerned Berry proved [2] that  $\Delta_3$  statistics display GOE or Poissonian form depending on whether the classical motion is fully chaotic or fully ordered. Although there is no formal proof that the NND is of the GOE type for chaotic systems, this suggestion [3] is now widely accepted and is supported by several numerical studies.

Fluctuation properties of the observed spectra of nuclei are in agreement with those of random matrices that belong

to the GOE [4–9]. This conclusion is based mainly on slow-neutron resonance data. These resonances lie several MeV above the yrast line in the region of high level density, where the complicated structure of the compound nucleus apparently justifies the use of random matrix theories.

Abul-Magd and Weidenmüller in 1985 evaluated [10] the spectral statistics of low-lying levels and concluded that states of a rotational character tend to deviate from GOE statistics. The suggestion of the pioneering work of Ref. [10], that the collective nuclear rotation introduces some type of regularity into the system, has gained further support in recent experimental investigations [11,12]. The NND of rotational states near the yrast line is very similar to the Poissonian form.

A theoretical investigation [13] in the low-spin region ( $I \leq 8$ ) using the algebraic interacting-boson model in the SU(3) dynamical symmetry limit also confirmed that rotational states behave more regularly. The spectral statistics of other limits of the interacting boson model and intermediate situations (vibrational and rotational coupling) [14–16,18] have been thoroughly investigated. For higher spins Alhassid and Vretenar [17] found that the Coriolis force increases the chaoticity, but that around  $I=16$ , due to the decoupling of the particles from the core and the alignment of their spins along the axis of rotation, the behavior of the system becomes more regular.

The effect of a rotation on chaotic motion has also been investigated in two-dimensional models. An interesting fact emerged from the study of rotating “billiards” [19–22]. It was shown that the cranking of the regular elliptic billiard introduces chaotic regions into the phase space whereas rotating a chaotic billiard leads to some regularity; i.e., the collective rotation can act in opposite ways in different systems: It can either increase or decrease the degree of chaoticity.

The appearance of chaos affects not only the statistical properties of the spectrum but also other quantities. It was

\*Permanent address: CLRC Daresbury Laboratory, Warrington WA4 4AD, UK.

shown in Ref. [22] that the dynamical moment of inertia for particles moving in a rotating elliptical billiard shows abrupt changes as a function of the rotational frequency. This phenomenon (often appearing as “back-bending”) is a common feature of the high-spin rotational states of nuclei. The observed irregularities in the case of the rotating billiard are associated with the coupling of the single-particle degrees of freedom to the collective motion through the Coriolis interaction. The most appropriate realistic nuclear models for studying this type of coupling are the cranking and particles-rotor models.

Our aim in this paper is to report on the differences in the spectral measures of these two models. This is an important point to consider, since the aim of making various approximations to the nuclear Hamiltonian is usually to obtain simplified calculations by throwing away certain symmetries. This may in turn have significant effects on the chaotic behavior of the system. For example, the BCS treatment of pairing forces describes a system that does not have good particle number. It is also specifically designed to give a good ground-state energy and is, therefore, unlikely to give the correct level spacings at high excitation energies. Its advantage of course is that it reduces the Hamiltonian to a mean-field problem for the resulting quasiparticles. The cranking approximation similarly neglects a two-body recoil term, again to obtain a mean-field problem. (See Ref. [23] for a discussion of the hierarchy of some of the approximations involved.)

Using the cranked Nilsson formalism an investigation of the appearance of chaos in rotating nuclei was carried out by Åberg [24], who applied a very schematic residual interaction (the absolute values of the two-body matrix elements were all taken to be the same and their signs were chosen randomly). The main point was to study how chaos appears for very high-spin states ( $I=50^+$ ) depending on the strength of the two-body force. Åberg was able to show that the onset of chaos affects a readily observable physical quantity: the average width of the  $E2$  strength function. In his work “good angular momentum states” were obtained from cranking calculations via an elaborate transformation to the laboratory system. (Actually these states do not have good angular momentum but only a fixed average projection along the cranking axis. This is somewhat analogous to the BCS problem mentioned above, where particle number is good only on the average.) The fluctuation properties of  $E2$  transitions in the cranking model was further investigated in Ref. [25] but without the transformation back to the laboratory system.

In what follows, therefore, we shall consider the particles-rotor Hamiltonian since this yields, in a natural way, states that have both good particle number and good spin. We shall then investigate the specific effects of the cranking approximation, while retaining a properly rotationally invariant description of the two-body forces and the deformed mean field. The major difference between these two approaches is essentially the neglect of the two-body recoil term. We shall see that this may have a rather large effect.

In this context, it is perhaps worthwhile making a few comments on the so-called Coriolis attenuation (see Ref. [26] and references therein) which is sometimes employed in the particle-rotor model in order to improve fits to experimental data. It is somewhat surprising that a correction appears to be

necessary in the model where the rotation is treated in a more fundamental way. However, the origin of this supposed correction arises from attempts to reduce an odd-particle-number system to one of a core plus a *single* particle (or quasiparticle). In this case the two-body component of the recoil term is absent and it is this which leads to the need for an attenuation of the Coriolis interaction. A detailed analysis of this point is given in Ref. [26]. In the present paper, we shall always consider there to be several particles outside the core and this problem will not then arise.

The appearance of chaos can now be analyzed experimentally using the high-spin states of nuclei thanks to high precision three-dimensional  $\gamma$ -ray correlation measurements and to a newly developed analyzing method [27–29]. This approach relies on a statistical analysis of electromagnetic transition rates. We shall extend our calculations to study this property in a future publication.

The outline of the paper is as follows. The particles-rotor and cranking models are reviewed in Sec. II. The methods of statistical analysis are described in Sec. III. The main emphasis in Sec. IV is the dependence of chaos on the total spin and on the cranking frequency, respectively. The effects of the core deformation, of the strength of the two-body force, and of the moment of inertia of the core are also investigated. Our conclusions are summarized in Sec. V.

## II. CRANKING AND PARTICLES-ROTOR HAMILTONIANS

We consider an even-even nucleus visualised as an axially symmetric rotor with a number of valence particles outside the core. The spin  $\vec{I}$  of the system is the sum of the angular momentum  $\vec{R}$  of the core and  $\vec{J}$ , the sum of the angular momenta of the particles. The total Hamiltonian of the particles-rotor model  $H_{PR}$  is the sum of a collective part and an intrinsic part  $H_{int}$ . The collective part  $H_{coll} = \vec{R}^2/2\Theta = (\vec{I} - \vec{J})^2/2\Theta$  consists of three terms  $H_{rot} + H_{recoil} + H_{Coriolis}$ . The pure rotational operator  $H_{rot} = (\vec{I}^2 - I_3^2)/2\Theta$ , the recoil term  $H_{recoil} = (J_1^2 + J_2^2)/2\Theta$ , and the Coriolis interaction  $H_{Coriolis} = -(I_1 J_1 + I_2 J_2)/\Theta$ , where  $\Theta$  is the moment of inertia of the core. The indices 1,2,3 refer to the body-fixed frame, where the three-axis is taken to be the symmetry axis. Note that the recoil term operates only on the valence particles and contains one-body and two-body terms if there is more than one particle outside the core. It thus has the same essential structure as  $H_{int}$  (see below).

For the intrinsic part of the Hamiltonian we take the form

$$H_{int} = \sum_{m,m'} V_{mm'}^{(def)} a_m^\dagger a_{m'} + \frac{1}{4} \sum_{m_1, m_2, m'_1, m'_2} V_{m_1 m_2 m'_1 m'_2}^{(1,2)} a_{m_1}^\dagger a_{m_2}^\dagger a_{m'_2} a_{m'_1}, \quad (1)$$

where  $a_m^\dagger$  and  $a_m$  are the one-particle creation and annihilation operators. Here we make the restriction that the particles can occupy only a single shell of  $j=13/2$  orbitals. For the residual two-body interaction  $V^{(1,2)}$  we choose a delta force

$-G \delta(\vec{r}_1 - \vec{r}_2)$ , which can be characterized by the single interaction strength  $G$ . Its two-body matrix elements are given by

$$\langle j^2 J || V^{(1,2)} || j^2 J \rangle = -\frac{1}{2} G (2j+1)^2 \begin{pmatrix} j & j & J \\ 1/2 & -1/2 & 0 \end{pmatrix}. \quad (2)$$

The particles also feel the presence of the core through a quadrupole mean field. The radial form factor of the deformed field is unimportant for a single  $j$  shell and the field can be characterized by the single parameter  $\kappa$  appearing in

$$\langle jm | V^{(\text{def})} | jm \rangle = -\kappa \frac{3m^2 - j(j+1)}{j(j+1)}. \quad (3)$$

(We omit the spherical part of the mean field and the kinetic energy of the particles since, in a single  $j$  shell, they simply add an overall constant energy to the spectrum.) The parameters of this model are then  $G, \kappa$ , and  $\Theta$ . They succinctly describe the competition between two-body forces, deformation, and the core rotation.

The eigenfunctions of the particles-rotor Hamiltonian are of the form

$$|\Psi_\alpha\rangle = \sum_K C_{\alpha K} |\phi_{MK}^I\rangle, \quad (4)$$

where the symmetrized basis states are defined by

$$|\phi_{MK}^I\rangle = \left( \frac{2I+1}{16\pi^2} \right)^{1/2} \{ D_{MK}^I(\Omega) \phi_K(\vec{r}'_1, \dots, \vec{r}'_N) + (-1)^{I+K} D_{M-K}^I(\Omega) \phi_{\bar{K}}(\vec{r}'_1, \dots, \vec{r}'_N) \}, \quad (5)$$

and primes denote positions with respect to the body-fixed axes (see, e.g., Ref. [23]). Here  $D_{MK}^I$  is the usual rotation matrix and  $\Omega$  describes the orientation of the core with respect to space-fixed axes. The  $N$ -body wave functions  $\phi_K(\vec{r}'_1, \dots, \vec{r}'_N)$  are antisymmetrized products of  $N$  single-particle states having good angular momentum projection  $K$  along the symmetry (intrinsic three-) axis. The state  $\phi_{\bar{K}}$  is obtained by rotating  $\phi_K$  through an angle  $\pi$  about the intrinsic one-axis. [For  $K=0$ , we may have  $\phi_{\bar{K}} = \pm \phi_K$ , when all the odd or even spin states vanish, respectively. The normalization of the wave function (5) then requires an extra factor of  $2^{-1/2}$ .]

In a much bigger space the diagonalization of the full many-particle matrix becomes prohibitive and many of the approximations discussed above are invoked, including cranking. We shall, therefore, within our present space, perform a cranking calculation to study its consequences. This simply involves a consideration of the Routhian or ‘‘energy in the rotating frame.’’ This may be written

$$H_{\text{cr}} = H_{\text{int}} - \omega \sum_{m,m'} \langle jm | j_1 | jm' \rangle a_m^\dagger a_{m'}, \quad (6)$$

where  $\omega$  is the cranking frequency and  $j_1$  is the one-component of the single-particle angular momentum. As with the full rotationally invariant Hamiltonian, the routhian

matrix will be diagonalized exactly. The results of these calculations will, therefore, correspond to cranking without mapping back to the laboratory frame referred to in the Introduction. The mapping back procedure used by [24] is considerably more tedious, since it involves the transformation  $I \approx I_1 = \langle J_1 \rangle + \omega \Theta$  (the corresponding laboratory energy is given in Ref. [23]). Since  $\langle J_1 \rangle$  is state dependent, one must vary the frequency for each state until all states yield the same (even then only average) spin values. This essentially means that one will end up studying spectral statistics by comparing energy levels which have been generated as the eigenstates of *different* Hamiltonians. We shall not present such results in this paper.

### III. EVALUATION OF SPECTRAL STATISTICS

The smooth part of the level density  $\bar{\rho}(E)$  is calculated using the Strutinsky averaging method [30] with curvature correction of order  $M$ , i.e.,

$$\bar{\rho}(E) = \frac{1}{\delta \pi^{1/2}} \sum_i L_M^{1/2} [(E - E_i)^2 / \delta^2] \exp[-(E - E_i)^2 / \delta^2], \quad (7)$$

where  $\delta$  is the energy-smoothing parameter and  $L_M^{1/2}$  is the generalized Laguerre polynomial. Having fixed  $M$  the energy-smoothing parameter is obtained by minimising the expression

$$\sum_{i=1}^{N-1} (X_i - i)^2, \quad (8)$$

with respect to  $\delta$ , where  $X_i$  are the unfolded energy levels:

$$X_i = \bar{N}(E_i), \quad i = 1, 2, \dots, N. \quad (9)$$

The smooth part of the cumulative level density is given by  $\bar{\rho}(E) = d\bar{N}(E)/dE$ . The level spacing is defined by

$$S_i = X_{i+1} - X_i, \quad i = 1, 2, \dots \quad (10)$$

Roughly speaking  $S_i$  is the original level spacing  $(E_{i+1} - E_i)$  in units of the local average level separation. The unfolding of the spectra can be carried out in a different way using

$$S_i = (E_{i+1} - E_i) \bar{\rho}(E_i), \quad i = 1, 2, \dots, N-1. \quad (11)$$

This unfolding of the spectra ensures that the average spacing in the series  $X_i$  is unity. In this way the fluctuation properties of the spectra of different systems can be compared. In our investigations both types of unfolding procedures led qualitatively to the same outcome. The results in the rest of the paper were produced using the mapping (9).

The first spectral statistics we use is the nearest neighbor distribution  $P(S)$ . The quantity  $P(S)dS$  gives the probability that the nearest neighbor of an arbitrarily selected level  $S_i$  lies in the interval  $(S_i + S, S_i + S + dS)$ . From the finite set of  $\{S_i\}_{i=1}^N$  only a histogram can be constructed as a NND. In order to have good statistics the bin size of the histogram is chosen to ensure that there are at least seven spacings in each bin. We considered the NND in the interval  $S \in (0, 2)$ .

Spectral statistics show Poissonian or GOE forms for integrable and fully chaotic systems. For mixed phase space systems the analytic forms of these statistics are not known. Different parametrizations have been suggested in the literature. We will use the following ones. Assuming that the ratio of the chaotic and ordered regions of the phase space is independent of the energy, it was suggested [31] that the NND should be parametrized in the form

$$P_{BR}(q,S) = \bar{q}^2 \exp(-\bar{q}S) \operatorname{erfc}\left(\frac{1}{2}\sqrt{\pi q}S\right) + (2q\bar{q} + \frac{1}{2}\pi q^3 S) \exp(-\bar{q}S - \frac{1}{4}\pi q^2 S^2), \quad (12)$$

where  $0 \leq q \leq 1$  is the measure of the chaotic region of the phase space and  $\bar{q} = 1 - q$ . Besides this Berry-Robnik parametrization (12) of the NND we shall also use the Brody distribution

$$P_B(b,S) = (1+b)AS^b \exp(-AS^{1+b}), \quad (13)$$

where

$$A = \Gamma\left(\frac{2+b}{1+b}\right)^{1+b} \quad (14)$$

and  $\Gamma$  denotes the usual gamma function. For fully chaotic and ordered systems  $q=b=1$  and  $q=b=0$ , respectively.

The spectral statistics  $\bar{\Delta}_3(L)$  measure the long-range correlation of the unfolded levels

$$\bar{\Delta}_3(X,L) = \min \frac{1}{L} \int_X^{X+L} [N_u(E) - (AE+B)]^2 dE, \quad (15)$$

where  $N_u$  is the cumulative level density of the unfolded levels  $X_i$ . We average  $\bar{\Delta}_3(X,L)$  over intervals  $(X, X+L)$  to get  $\bar{\Delta}_3(L)$ , as outlined in [3]. For ordered systems  $\bar{\Delta}_3(L) = L/15$  and for fully chaotic ones  $\bar{\Delta}_3(L) \approx \ln(L)/\pi^2 - 3/4$  for  $L \gg 1$ . The explicit calculation of the spectral rigidity was done with the method described in [32].

Using the same arguments as in Ref. [31] for the NND a mixed statistics for the spectral rigidity was derived [33]. This reads

$$\bar{\Delta}_3(q,L) = \Delta_3^p(qL) + \Delta_3^{\text{GOE}}((1-q)L). \quad (16)$$

The  $b$  and  $q$  parameters of the NND distributions and the spectral rigidity are determined by least-squares fits to the numerical results. The errors in the best-fit values of these parameters were estimated by the method of maximum likelihood and the use of constant chi-squared boundaries as a confidence limit [34]. We will not draw error bars on the figures but it could be understood that the relative error of the estimated parameter values is about 10% throughout.

#### IV. RESULTS

In all of our calculations six particles were put in a single  $i_{13/2}$  orbit. (Six and eight are the even particle numbers that give the maximum number of many-particle states in this problem.) The statistical analyses were carried out using states with a given spin in the particles-rotor model. In the analysis of the cranking model results, the statistics were

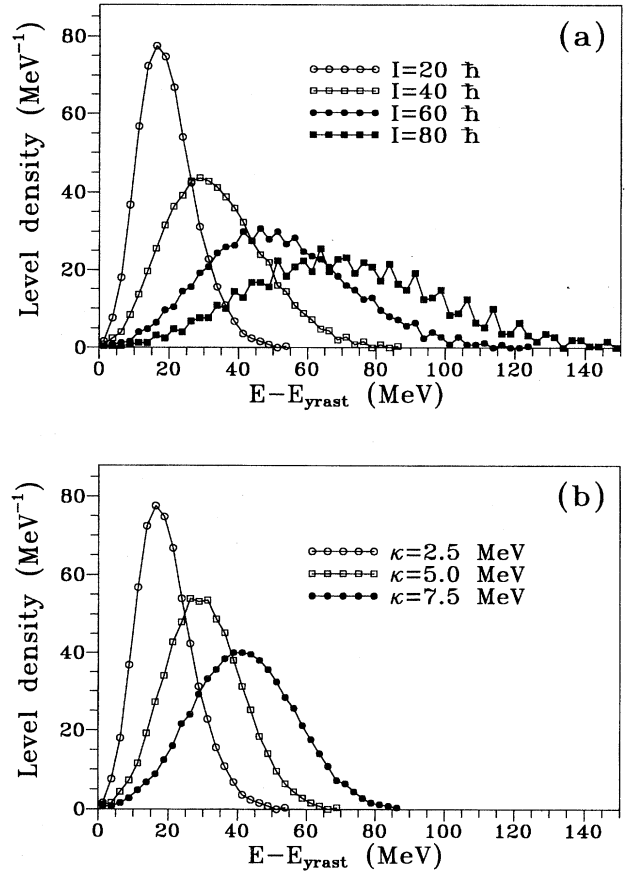


FIG. 1. (a) The level density corresponding to our standard parameter set is shown for the spin values indicated. The energy is taken relative to the yrast level for the appropriate spin. (b) Same as (a) but for  $I=20$  with various values of the deformation parameter  $\kappa$ . Note the roughly Gaussian shape of the curves and the increasing energy spread as either  $I$  or  $\kappa$  is increased.

determined for fixed cranking frequency and signature (i.e., symmetry of the states with respect to a rotation of  $\pi$  around the cranking axis). Since signature is a good quantum number, we considered only those states with the same signature as the ground state. Unless stated otherwise we used the following “standard” parameter values in the calculations:  $G = G_0 = 0.45$  MeV,  $\Theta = \Theta_0 = 24 \hbar^2$  MeV $^{-1}$ , and  $\kappa = \kappa_0 = 2.5$  MeV. Similar parameters have frequently been used in the literature and are thought to be reasonable in this model [26,35]. (This pairing strength is of course somewhat larger than its usual value. The reason for this is that the level density of the single  $j$  shell is lower than in a realistic calculation containing many shells. The above value of  $G$  compensates for this and still yields “two-quasiparticle” energies and crossing frequencies with approximately their experimental values.)

In Fig. 1(a) we show the level densities produced by our standard parameters for various values of the spin. The energies are taken relative to the appropriate yrast states. It can be seen that at low energies the level density increases rapidly, as one would expect. At higher energies, however, the level density falls off again, giving a roughly Gaussian curve which becomes significantly broader at high angular mo-

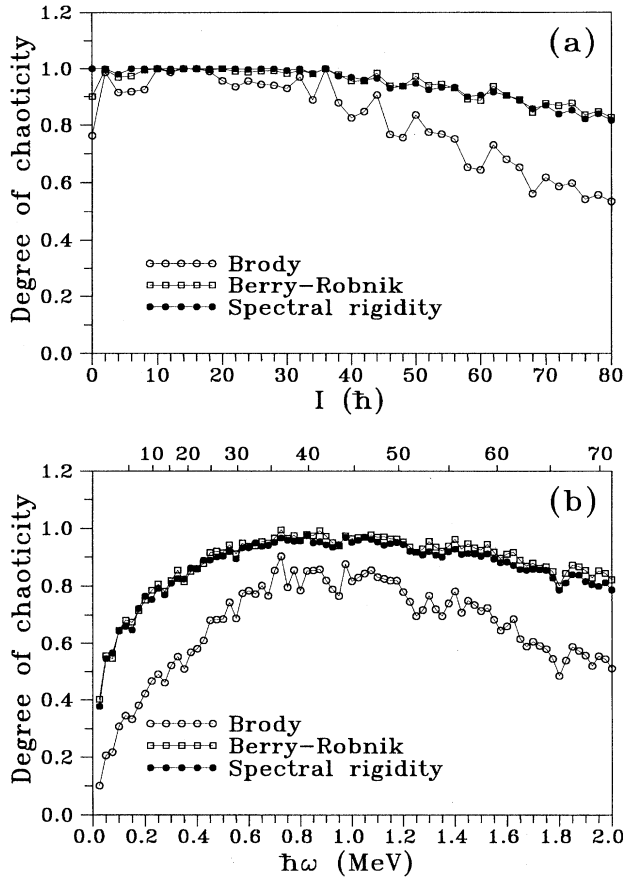


FIG. 2. The best-fit parameters for the degree of chaoticity with mixed statistics are shown for (a) the particles-rotor model and (b) the cranking model as functions of spin and cranking frequency, respectively. Both calculations use our standard parameter set. The NND is analyzed with both the Berry-Robnik (squares) and Brody (circles) parametrizations. On the top of the lower figure, we show the values of  $\langle I_1 \rangle$  for the yrast state at the corresponding frequencies. As mentioned in the text, the relationship between these two quantities is not linear, due to particle alignments.

menta. The above falloff is unphysical but must occur in our model due to the finite single-particle space we employ. (Such a basis is of course necessary if one wishes to perform an exact diagonalisation of the Hamiltonian.) For high even angular momenta (signature +1) the total basis size is 1519. This number is smaller for  $I < 24$  since for these spins, not all values of  $K$  are possible; e.g., for  $I=20$  one has 1512 states and this falls to just the 93 positive signature  $K=0$  states for  $I=0$ . In the cranking calculation the basis size is of course independent of  $\omega$  and always contains all 1519 configurations. In our subsequent statistical analyses, all of the allowed configurations are taken into account, except in Fig. 5(b) where the spectral rigidity is considered for sets of 100 levels of increasing energy.

Fig. 1(b) shows the level density for  $I=20$  with  $\kappa = \kappa_0$ ,  $2\kappa_0$ , and  $3\kappa_0$ . Again a roughly Gaussian shape is obtained whose width increases with increasing deformation.

The calculated NND's were fitted both with the formulas (12) and (13). In Figs. 2(a) and 2(b) we show the best-fit

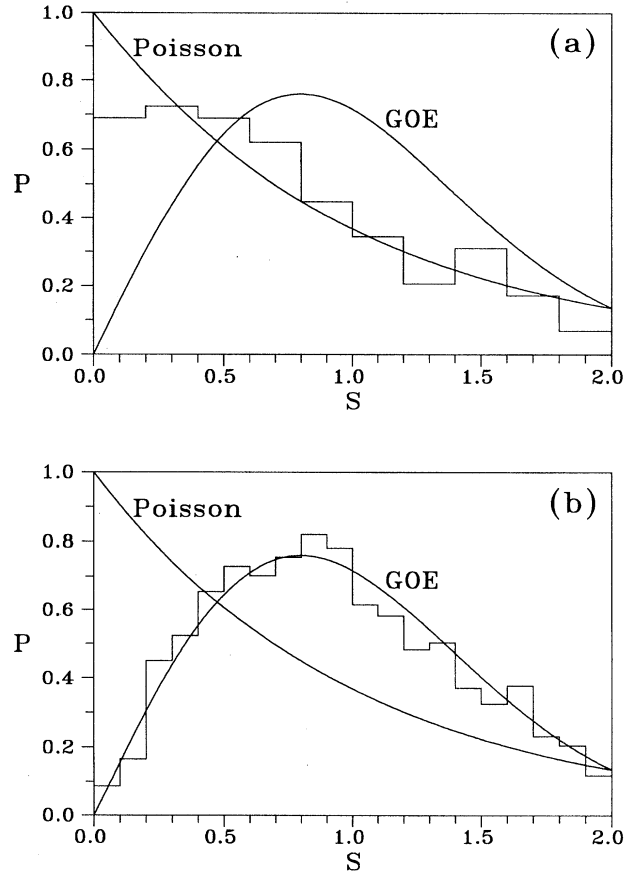


FIG. 3. The nearest-neighbor distributions are shown for (a) states of the intrinsic Hamiltonian with  $K=2^+$  and (b) states of the particles-rotor Hamiltonian with  $I=20^+$ .

Brody and Berry-Robnik parameters as functions of the spin and cranking frequency. Our observation from this and a series of other calculations (not shown here) is that the Berry-Robnik parametrization shows a greater degree of chaoticity than the Brody distribution (though bear in mind that interpreting the parameters  $b$  and  $q$  as the degree of chaoticity is a great simplification). Although the quantitative predictions for the degree of chaoticity are quite different for the two parametrizations, the qualitative behavior was the same in each of the cases we studied. In the Berry-Robnik prescription one may define the chaoticity using either the NND or the spectral rigidity and it is reassuring to note that the same degree of chaoticity is predicted by both of these measures. For the rest of the paper we shall, however, in common with most of the current literature, simply use the NND statistics of the Brody parametrization.

To understand our nuclear model it is instructive to look first at the situation where the valence particles are not coupled to the rotor, i.e., to look at the spectrum of the intrinsic Hamiltonian  $H_{\text{int}}$  of Eq. (1) alone. The projection  $K$  of the spin on the three-axis of the body-fixed system is now a good quantum number. In Fig. 3(a) we show the NND for the states with  $K=2$ . It turns out that the spectrum of the intrinsic Hamiltonian exhibits reasonably ordered behavior as long as  $G/G_0 < 1.4$ . However, the ordered NND com-

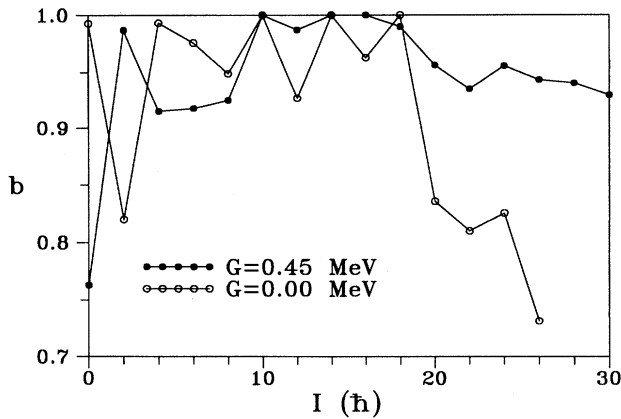


FIG. 4. The degree of chaoticity (best-fit parameter of the Brody distribution) is given as a function of spin for the particles-rotor model. The solid circles show the case where the two-body interaction is turned off. The open circles show the results for  $G = G_0 = 0.45$  MeV.

pletely changes if the particles are coupled to the rotor. Figure 3(b) displays the NND for the states with  $I = 20^+$ . Here a GOE distribution clearly prevails.

To further emphasize the importance of the two-body terms from the rotational coupling, we may switch off the “real” two-body interaction between the valence particles. Figure 4 shows that the angular momentum fluctuations have a profound effect on the NND. The degree of chaoticity at low spins is influenced mainly by the coupling to the core and the effect of the two-body interaction is of secondary importance.

In the low-spin regime ( $I < 20$ ) the particles-rotor system exhibits GOE behavior, i.e., the system is chaotic. Increasing the value of the spin, the system gradually becomes more ordered [see, for example, Fig. 2(a)]. This can also be seen from Fig. 5(a), where the spectral rigidity is displayed for different spin values. This behavior is due to the decoupling of the particle spins from the deformation axis of the rotor and their alignment along the rotation axis which tends to make the system more regular.

The effect of the excitation energy on the degree of chaoticity is shown by the spectral rigidity of Fig. 5(b). Analyzing the whole energy range for states with  $I = 80^+$  we find relatively regular behavior. However, dividing the energy scale into different regions we find that the chaoticity increases with increasing excitation energy. The analyses were carried out using groups of one hundred levels of increasing energy.

In Fig. 6 we show the dependence of chaoticity on the parameter  $G$ . We see that the larger the two-body interaction strength relative to the deformation energy, the larger the chaoticity. This is true in both models. There is a significant difference between the cranking and the particles-rotor models when  $G$  is very small and in general when the spin is small. Consider switching off the two-body interaction between the valence particles i.e., taking  $G = 0$ . Åberg found [24] that in this case the cranking model exhibits regular behavior. This agrees with our finding [see Fig. 6(b) and remember the error in the best-fit parameter]. However, from

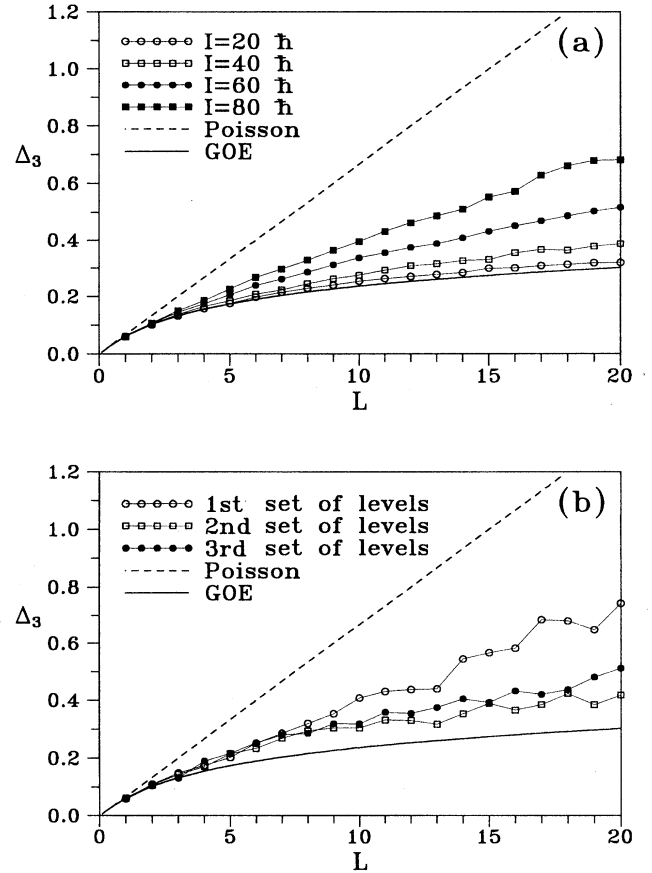


FIG. 5. The spectral rigidity of the particles-rotor Hamiltonian is presented for different values of (a) the spin and (b) for different regions of energy. The first set of energy levels is the first hundred, the second set is the next hundred, etc., in order of increasing energy.

Fig. 6(a) we see that the particles-rotor system exhibits regular behavior only for very high spins.

The explanation of our finding is that in the cranking model the spin is not a good quantum number, whereas in the particles-rotor model rotational symmetry is preserved due to the Coriolis and the recoil terms. However, the recoil term  $(J_1^2 + J_2^2)/2\Theta$  contains two-body operators, and so there is always an “interaction” between the particles, even if the real two-body force is switched off. The regular behavior that was found in [24] turns out to be an artifact of the cranking Hamiltonian for which the recoil term is absent. However, the results of [19–22], where *free* particles were moved in a rotating two-dimensional billiard (i.e., also a cranking calculation with no two-body forces), yield a mixed phase space, and so this situation is not entirely clear.

Fixing the two-body strength at our standard value of  $G_0 = 0.45$  MeV, we next varied the deformation parameter. The results are shown in Fig. 7. For large  $\kappa$  an increase in regularity can be observed at lower spins (or at lower cranking frequencies) relative to smaller  $\kappa$  values. This finding may be understood using similar arguments as those of Ref. [36]. The higher the  $\kappa$ , the better the quantum number  $K$  is conserved. The suppression of the chaos arises from a partially valid symmetry. (It is interesting to note that at higher

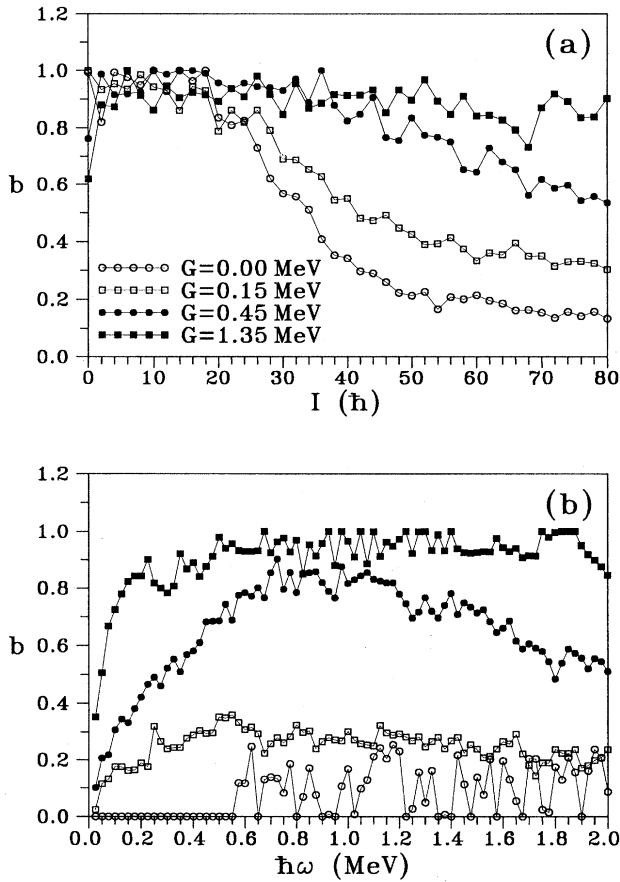


FIG. 6. The degree of chaoticity is plotted as a function of (a) the spin and (b) the cranking frequency for different values of the two-body interaction strength  $G$ . Note the very large differences between the two models for slow rotations independent of  $G$ .

spins in the rotor model, the degree of chaoticity becomes independent of  $\kappa$  rather quickly. For cranking, however, this “convergence” is somewhat slower.)

In the particles-rotor model one should also investigate the effect of the moment of inertia. From general grounds it is expected that for very large moments of inertia the particles-rotor model should yield very similar results to the cranking description. Figure 8 confirms this expectation for the spectral statistics. Our previous observation (the larger the spin the smaller the chaoticity), however, holds only for smaller values of  $\Theta$  and the opposite trend prevails for large moments of inertia. This behavior can, however, be easily understood. Increasing  $\Theta$  to large values has essentially two main effects. First, it will kill off the recoil term which varies as  $1/\Theta$  (this essentially turns the particles-rotor model into cranking). Second, for a fixed spin, the effective frequency decreases as  $\Theta$  increases, since  $\omega \approx I/\Theta$ . Thus (except at  $I=0$ , where the system appears to remember that it is a particles-rotor calculation) the large- $\Theta$  results of Fig. 8 tend to the low- $\omega$  behavior of Fig. 2(b).

The above jump in chaoticity at  $I=0$  [which is also evident in Fig. 7(a)] can be understood in the following way. The intrinsic Hamiltonian has good  $K$  and we have already seen [Fig. 3(a)] that separating out the good- $K$  states gives a

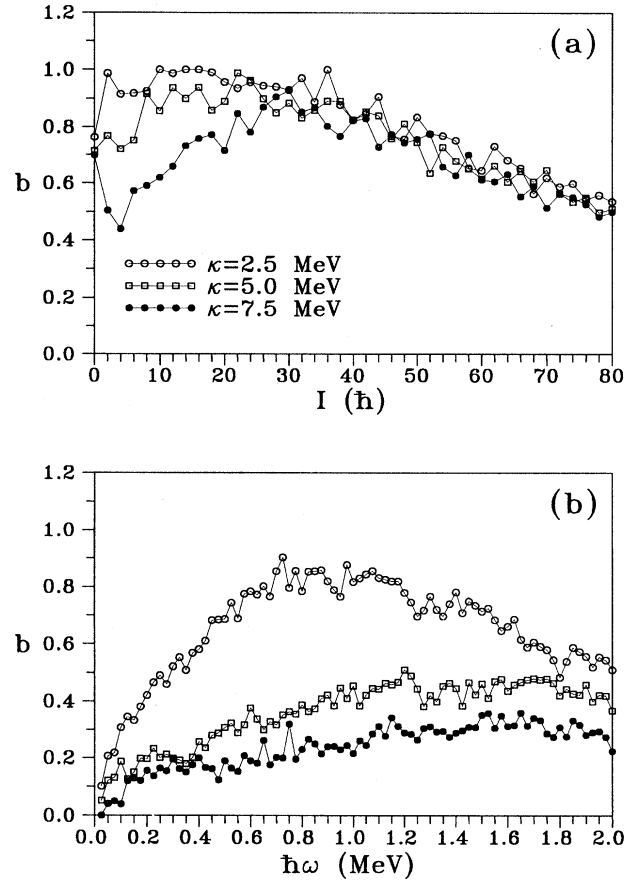


FIG. 7. The degree of chaoticity is depicted as a function of (a) the spin and (b) the cranking frequency for different values of the quadrupole deformation parameter  $\kappa$ . In the particles-rotor case the high-spin results rapidly become independent of deformation.

reasonably ordered spectrum. This is, however, least true of the low- $K$  states (especially  $K=0$ ) which are most affected by the pairing force. In the particles-rotor calculation,  $I$  is a good quantum number and the basis for a given  $I$  includes only those intrinsic states with  $K \leq I$ . Thus as  $I$  becomes small, the relative importance of the more “chaotic”  $K=0$  states increases. Hence the jump in chaoticity at  $I=0$ . For the cranking calculation, however, all  $K$  values are included for all  $\omega$ . (This is an intrinsic property of cranking rather than anything special about the present calculations.) The cranking results, therefore, give less weight to the low- $K$  states and remain regular even down to  $\omega=0$ . Thus it is rather dangerous to use a cranking calculation to investigate statistical properties in this low-spin regime.

## V. CONCLUSIONS

A systematic study of the appearance of chaos in two reasonably realistic models, capable of qualitatively describing many of the features of nuclear high-spin states, has been carried out. It is known that the two-body interaction strength plays an important role in the appearance of chaotic motion [24,37]. The present study, however, reveals that the recoil coupling to the core allows angular momentum fluc-

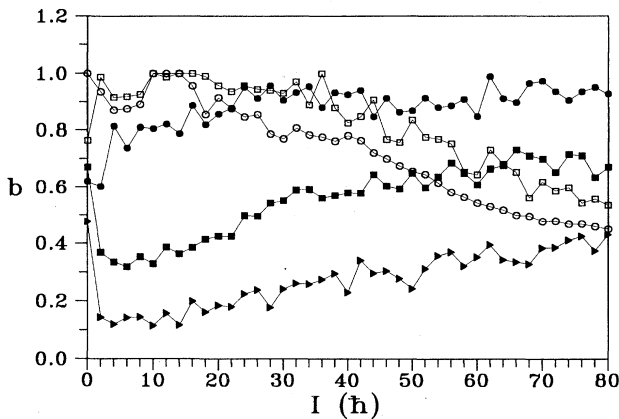


FIG. 8. The degree of chaoticity is displayed as a function of spin for different values of the moment of inertia  $\Theta$ . The results for  $\Theta = 8, 24, 72, 216,$  and  $648\hbar^2 \text{ MeV}^{-1}$  are indicated by open circles, open squares, solid circles, solid squares, and solid triangles, respectively.

tuations that lead to chaotic spectral statistics even if the “true” two-body force is negligible. Indeed at low spins this coupling principally determines the degree of chaoticity, and so cranking results in this region should be viewed with some caution. Of course our calculations have been performed in a somewhat restricted single-particle basis but it is unlikely that these conclusions regarding the use of cranking would be qualitatively changed by increasing this space.

There are, however, some effects due to the use of this relatively small basis which deserve further comment. It is clear from Fig. 1(b) that an increasing deformation leads to a

lower level density at low excitation energies by broadening the energy spread. In a similar fashion, a divergence of levels is brought about by the rotation [see Fig. 1(a)]. This in itself does not alter our conclusions regarding the degree of chaoticity, since the nearest-neighbor distributions are always expressed relative to the local average spacing (see Sec. III). However, in a more physical space, the level density will remain more constant because the diverging levels from the single shell that we consider will tend to be replaced by levels intruding from other shells. This shell mixing may have significant additional effects on the degree of chaoticity.

From the study of the particles-rotor model we can conclude that a large quadrupole deformation suppresses chaos at low spins and that at higher spins it has relatively little effect. The cranking calculation also shows the trend of the suppression of the chaoticity due to the large quadrupole deformation. There is, however a delicate balance between the competition of the different effects. Increasing the moment of inertia is capable of reversing the above trend.

Fixing the model parameters around standard values we have found, in agreement with algebraic models, that due to the Coriolis interaction, the degree of chaoticity decreases with increasing spin. We conclude that chaos is more pronounced for normal deformations and low spins (where cranking is poor) than for superdeformations and high spins.

#### ACKNOWLEDGMENTS

The authors are grateful for support from the Hungarian OTKA Grant No. 3010 and from a Royal Society exchange agreement.

- [1] M. V. Berry and M. Tabor, Proc. Roy. Soc. London A **356**, 375 (1977).
- [2] M. V. Berry, Proc. Roy. Soc. London A **400**, 229 (1985).
- [3] O. Bohigas, M. J. Giannoni, and C. Schmit, Phys. Rev. Lett. **52**, 1 (1984).
- [4] C. E. Porter, *Statistical Theories of Spectra: Fluctuations* (Academic Press, New York, 1965).
- [5] T. A. Brody, J. Flores, J. B. French, P. A. Mello, A. Pandey, and S. S. M. Wong, Rev. Mod. Phys. **53**, 385 (1981).
- [6] R. U. Haq, A. Pandey, and O. Bohigas, Phys. Rev. Lett. **48**, 1086 (1982).
- [7] O. Bohigas, R. U. Haq, and A. Pandey, in *Nuclear Data for Science and Technology*, edited by K. H. Böckhoff (Reider, Dordrecht, 1983), p. 809.
- [8] O. Bohigas, R. U. Haq, and A. Pandey, Phys. Rev. Lett. **54**, 1645 (1985).
- [9] G. E. Mitchell, E. G. Bilpuch, P. M. Endt, and J. F. Shriner, Jr., Phys. Rev. Lett. **61**, 1473 (1988).
- [10] A. Y. Abul-Magd and H. A. Weidenmüller, Phys. Lett. **162B**, 223 (1985).
- [11] J. D. Garrett, J. R. German, L. Courtney, and J. M. Espino, in *Proceedings of the International Conference on Future Directions in Nuclear Physics with 4 $\pi$ -Gamma Detection Systems of the New Generation*, Strasbourg, 1991, edited by J. Dudek and B. Haas, AIP Conf. Proc. No. 259 (AIP, New York, 1992), p. 345.
- [12] J. D. Garrett, in *Proceedings of the 8th International Symposium on Capture Gamma-Ray Spectroscopy and Related Topics*, Fribourg, Switzerland, edited by J. Kern (World Scientific, Singapore, 1994), p. 494.
- [13] V. Paar and D. Vorkapić, Phys. Lett. B **205**, 7 (1988).
- [14] V. Paar and D. Vorkapić, Phys. Rev. C **41**, 2397 (1990).
- [15] Y. Alhassid, A. Novoselsky, and N. Whelan, Phys. Rev. Lett. **65**, 2971 (1990).
- [16] Y. Alhassid and N. Whelan, Phys. Rev. Lett. **67**, 816 (1991).
- [17] Y. Alhassid and D. Vretenar, Phys. Rev. C **46**, 1334 (1992).
- [18] N. Whelan and Y. Alhassid, Nucl. Phys. A **556**, 42 (1993).
- [19] D. B. Fairlie and D. K. Siegart, J. Phys. A **21**, 1157 (1988).
- [20] D. K. Siegart, J. Phys. A **22**, 3537 (1989).
- [21] H. Frisk and R. Arvieu, J. Phys. A **22**, 1765 (1989).
- [22] A. J. S. Traiber, A. J. Fendrik, and M. Bernath, J. Phys. **23**, L305 (1990).
- [23] D. M. Brink, B. Buck, R. Huby, M. A. Nagarajan, and N. Rowley, J. Phys. G **13**, 629 (1987).
- [24] S. Åberg, Phys. Rev. Lett. **64**, 3119 (1990); Prog. Part. Nucl. Phys. **28**, 11 (1992).
- [25] M. Matsuo, T. Dössing, B. Herskind, and S. Frauendorf, Nucl. Phys. A **564**, 345 (1993).
- [26] N. Rowley and K. F. Pál, in *Proceedings of the International*



- Conference on Future Directions in Nuclear Physics with  $4\pi$ -Gamma Detection Systems of the New Generation*, Strasbourg, 1991, edited by J. Dudek and B. Haas, AIP Conf. Proc. No. 259 (AIP, New York, 1992), pp. 463–476, and references therein.
- [27] B. Herskind, T. Døssing, S. Leoni, M. Matsuo, and E. Vigezzi, *Prog. Part. Nucl. Phys.* **28**, 235 (1992).
- [28] B. Herskind, T. Døssing, D. Jerrestam, K. Schiffer, S. Leoni, J. Lisle, R. Chapman, F. Khazaie, and J. N. Mo, *Phys. Lett. B* **276**, 4 (1992).
- [29] B. Herskind, A. Bracco, R. A. Broglia, T. Døssing, A. Ikeda, S. Leoni, J. Lisle, M. Matsuo, and E. Vigezzi, *Phys. Rev. Lett.* **68**, 3008 (1992).
- [30] P. Ring and P. Schuck, in *The Nuclear Many-Body Problem, Texts and Monographs in Physics* (Springer-Verlag, New York, 1980), p. 83.
- [31] M. V. Berry and M. Robnik, *J. Phys. A* **17**, 2413 (1984).
- [32] O. Bohigas and M.-J. Giannoni, in *Mathematical and Computational Methods in Nuclear Physics*, Vol. 209 of *Lecture Notes in Physics*, edited by J. S. Dehesa, J. M. G. Gomez, and A. Polls (Springer-Verlag, Berlin, 1984), p. 1.
- [33] T. H. Seligman and J. J. M. Verbaarschot, *J. Phys. A* **18**, 2227 (1985).
- [34] S. T. W. H. Press, B. P. Flannery, and W. Vetterling, *Numerical Recipes* (Cambridge University Press, Cambridge, England, 1986).
- [35] C. G. Andersson and J. Krumlinde, *Nucl. Phys.* **A334**, 486 (1980).
- [36] N. Whelan, Y. Alhassid, and A. Leviatan, *Phys. Rev. Lett.* **71**, 2208 (1993).
- [37] M. Matsuo, T. Døssing, E. Vigezzi, and R. A. Broglia, *Phys. Rev. Lett.* **70**, 2694 (1993).